

POWER SUPPLIES BASED FULL-BRIDGE LLC RESONANT CONVERTER PERFORMANCE FOR IH APPLICATIONS

Ala HOUAM¹

Echahid Cheikh Larbi Tebessi University, Algeria

Rabah DAOUADI

Echahid Cheikh Larbi Tebessi University, Algeria

Zoubir AOULMI²

Echahid Cheikh Larbi Tebessi University, Algeria

Adel DJELLALI

Echahid Cheikh Larbi Tebessi University, Algeria

Abstract:

This paper describes the analysis and performance of a full-bridge LLC resonant converter based on power supplies for IH applications. The analysis contains five components: half bridge inverter, resonant tank, high frequency transformer, rectifier and coil. The switching bridge generates a square waveform to excite the LLC resonant tank, which will produce a resonant sinusoidal current which is transferred to the secondary of the converter through a high-frequency transformer. As it scales the voltage up or down according to the output requirements. The load represented by the equivalent circuit of the coil and work-piece is fed by the current transformed by the rectifiers.

Considering that load parameters and resonant frequency vary greatly in all phases of system operation, this paper provides improved knowledge of output power control for high temperature applications.

The validity of the analyzed converter parameters had been simulated and tested using MATLAB-SIMULINK software.

The results of testing demonstrated that the proposed scheme and assembly has good efficiency, and it is well suited for magnetic induction heating systems.

Keywords: *Full-Bridge Inverter, LLC Circuit, Resonant Tank, Induction Heating, Rectifier.*

 <http://dx.doi.org/10.47832/2717-8234.16.10>

¹  a.houam@univ-tebessa.dz

²  zoubir.aoulmi@univ-tebessa.dz



1. Introduction

With scientific advances, the focus is now on finding solutions to meet the challenges posed by new commercial applications, especially in the current economic context. Due to advances in power electronics [1], and magnetic materials science, heat treatment has made significant progress.

Induction heating is one of the most effective methods of energy conversion from the electrical to thermal form [2,3], used in diverse industrial processes such as preheating furnaces, heat treatments, welding, brazing, melting, etc [4,5]. It is thought to be more effective than other heating methods, such as resistance heating, because heat is generated directly within the workpiece during the induction heating process, as opposed to resistance heating, which first heats the heating element before transferring heat to the workpiece through conduction, which takes longer and ultimately results in more heat loss. Moreover, it involves three successive stages of physical phenomena:

- The transfer of energy from the inductor to the object to be heated through electromagnetic induction;
- The conversion of this energy into heat in the object by the Joule effect;
- The transmission of heat through the object by conduction, convection and thermal radiation, thus allowing its propagation and its transfer to other surrounding elements.

Induction heating depends mainly on the frequency of the alternating current used, the design of the inductor and the quality of the magnetic coupling. The frequency of the current determines the depth of heat penetration, and the austenitizing temperature can usually be reached within seconds when heating by induction.

Various power switching architectures and control techniques exist, such as ZVS control mode [6], phase shift control (PSC) [7,8] which is based on variation of output power by shifting the phase of the switch conduction sequences, Single-ended voltage cancellation (AVC) [9] where the control is based on voltage-cancellation for conventional fixed-frequency, the asymmetrical duty-cycle (ADC) control technique [10] which employs an unequal duty-cycle operation of the switches in the converter and DC- density modulation control Pulses (PDM) [11].

LLC resonant converters offer a very efficient solution for induction heating. As proven by studies [12,13,14]. These are an electronic circuits that exploit resonance in series or parallel configurations to reduce electrical and thermal stresses on switches, minimize harmonics and limit switching losses. They make operation at moderate and high frequencies easier by smoothly commutating the interrupters.

In this work, the aim of this study is to analyze the power supply of induction heating systems using resonant converters.

2. Basic principle of induction heating

The induction heating concerns the electromagnetic theory; Michael Faraday

discovered that the alternating current flowing through the coil makes the magnetic field around the coil, the induced electromotive force in a closed loop equals the negative of the time rate of change of the magnetic flux through the loop [15].

$$E = -N \frac{d\Phi_R}{dt} \quad 01$$

Where:

E: electromotive force

N: the magnetic flux

Φ : number of turns

When the loop is short-circuited, the induced voltage E will cause the appearance of a short-circuit current flowing in the opposite direction to the phenomenon that creates it, as stipulated by the Faraday-Lenz law as shown in Figure 1 (a,b).

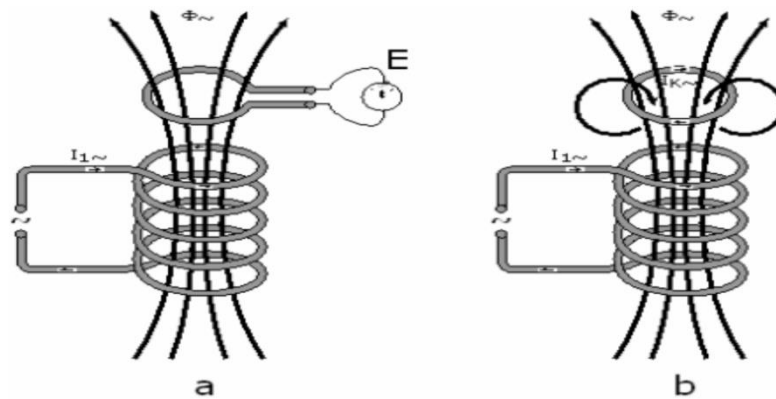


Figure 1 Faraday's law [14]

This EMF generates an alternating current (eddy current). Then, the basic principle of IH system is based on the creation of an eddy current within the workpiece when a conductive element is immersed in a variable magnetic field [16], the restriction of these currents due to the resistance of the material dissipates the energy and generates heat in the workpiece as shown in Figure 2.

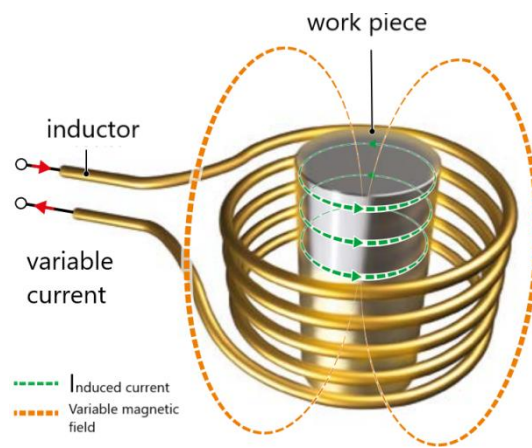


Figure 2. Basic principle of IH

The principle of electromagnetic induction heating is based on two physical phenomena:

- Electromagnetic induction.
- Joule effect.

2.1. Circuit Description

The circuit consist five parts; the switching bridge (inverter) [17], the resonant tank, a high frequency transformer, a rectifier and a load (coil+workpiece)

The full bridge LLC tank consists of two resonant inductors, a series inductor (L_r) and a magnetizing inductor (L_m), a resonant capacitor (C_r) and an induction coil that comprises a series combination of a resistor (R_{eq}) and an induction coil inductor (L_{coil}) [18].

The main power circuit features of a full bridge LLC resonant converter is illustrated in Figure 3.

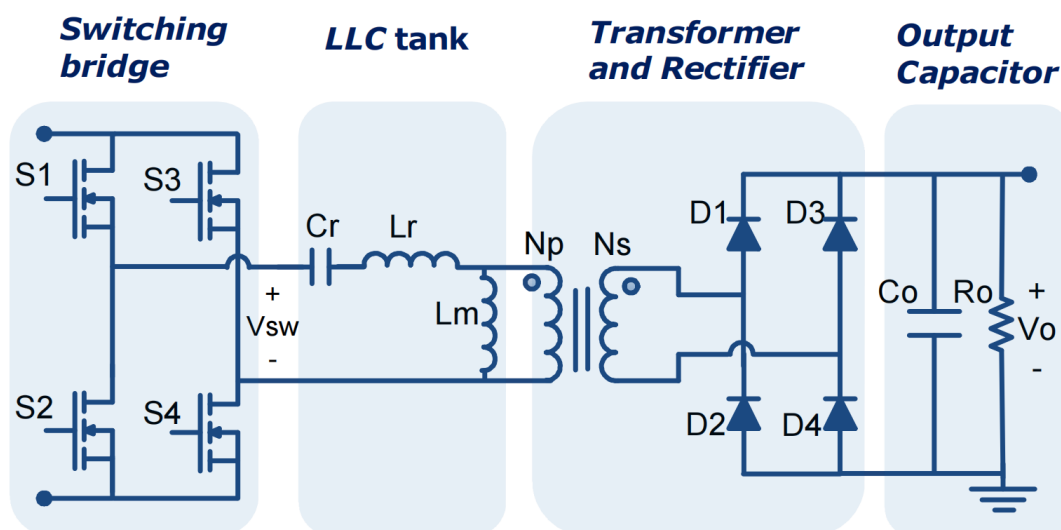


Figure 3. Full bridge LLC resonant converter

The interaction of these components generates an electromagnetic field which induce s heat by induction. Key parameters such as inverter frequency, amperage and load geometry are analyzed to optimize energy efficiency and ensure even heat distribution.

The switching bridge switches and converts the DC voltage to excite the LLC resonant tank. This last then enters the resonant tank, which eliminates the square wave harmonics and produces a sine wave with the fundamental frequency as the output.

$$\frac{di_{Lr}}{dt} = \frac{1}{L_r}(V_{in} - V_{cr} - V_{Lm}) \quad 2)$$

$$\frac{dV_{cr}}{dt} = \frac{i_{Lr}}{C_r} \quad 3)$$

$$\frac{dV_0}{dt} = N(i_{Lr} - i_{Lm}) - \frac{V_0}{R_{eq}} \quad 4)$$

$$\frac{di_{Lm}}{dt} = \frac{V_{Lm}}{L_m} \quad 5)$$

Where: i_{Lr} , i_{Lm} and v_{cr} are the resonant inductor current, the resonant capacitor voltage, and the magnetizing current, respectively. v_{Lm} is the voltage of L_m , and N is the transformer turns ratio.

According to another way of designating resonant converters, the LLC resonant belongs to the family of multi-resonant converters [15]. Actually, there are two resonant frequencies associated to this circuit f_r and f_m . the first is related to the series resonant elements L_r and C_r as in Eq. (6).

$$f_r = \frac{1}{2\pi\sqrt{L_r \times C_r}} \quad 6)$$

And when the resonant elements L_r and C_r resonate with the parallel resonance element L_m . here, new frequency f_s is provided as in Eq. (7).

$$f_s = \frac{1}{2\pi\sqrt{(L_r + L_m) \times C_r}} \quad 7)$$

3. SIMULATION MODEL

Using Simulink /MATLAB software, we have created the assembly of Figure 5 which represents the block diagram of full bridge LLC resonant converter, and then created a control circuit to obtain the command signal (S1 and S2) to control the MOSFETs (M1 and M2) as shown in Figure 6. In order to validate and test our assembly, we used the different parameters which are shown in the Table 1.

Table 1. . Parameters of the LLC resonant converter

Item	Symbol	Value
Input Voltage	V_{in}	400V
Switching Frequency	f_r	40kHz
Parallel resonant capacitor	C_r	0.1 μ F
resonant inductor	L_r	22.6 μ H
magnetizing inductor	L_m	80 μ H
Equivalent resistor (with workpiece)	R_{eq}	25 Ω
Equivalent inductor	L_{eq}	1.2 μ H
Switch Frequencies		
Case 01	f_s	40kHz
Case 02	f_s	10kHz
Case 03	f_s	100kHz

In order to control the MOSFETS (M1, M3, M4, and M2), we first assembled the block diagram of the Full-bridge LLC resonant converter, and then we built a control circuit to get the control signal (S1 and S2) as shown in figure 4,

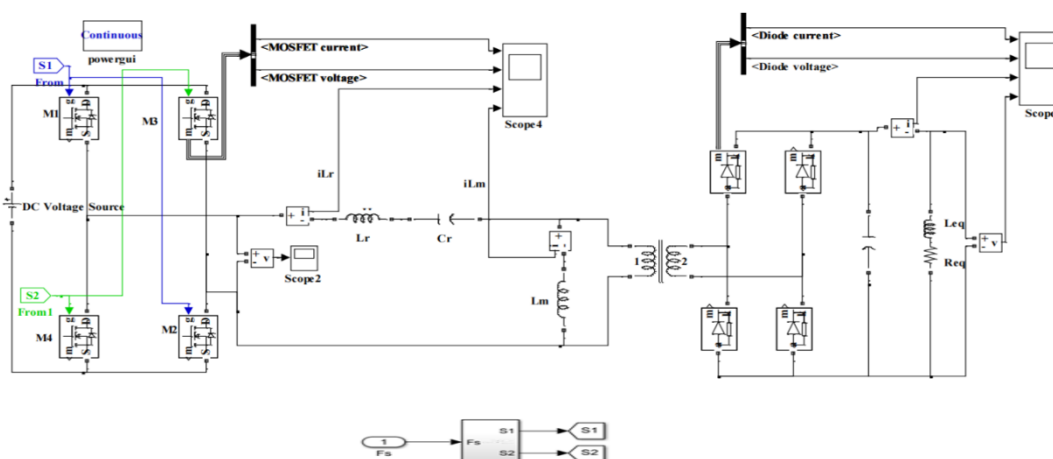


Figure4. Simulation model of full bridge LLC resonant converter ($f_s=f_r$)

4. RESULTS AND DISCUSION

Case of $f_s=f_r$

The following figures shows the command signal (S1 and S2) to control the MOSFETs (M1 and M2) at the top and bottom of the half-bridge converter respectively. While applying the gating pulse to the MOSFET it is necessary to take care of the overlapping of ON time

and OFF time of two semiconductor switches. If 2nd MOSFET is given the pulse before the prior one is not completely OFF, it may cause short circuit and thus failure of the semiconductor device. Therefore the control of this switches must be complementary.

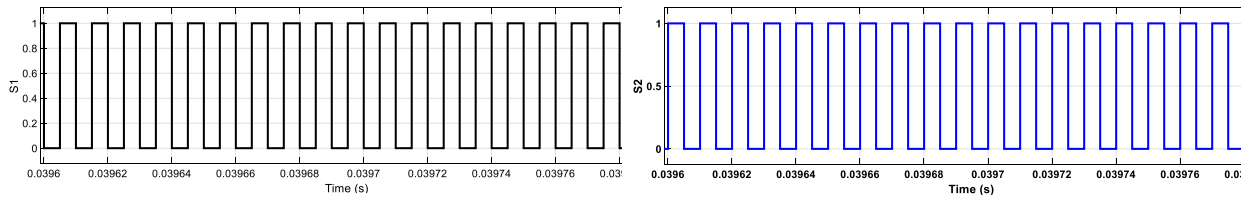


Figure 5. Signals generated for the control of a full-bridge inverter

The voltage and current waveforms at switch 1 at the converter's top are depicted in Figure (IV.4). When the switch is blocked, the voltage equals the 400 volts of the DC supply; otherwise, it equals zero volts, and the current is about 10 amperes. The switch's changing of states causes the emergence of the negative current component.

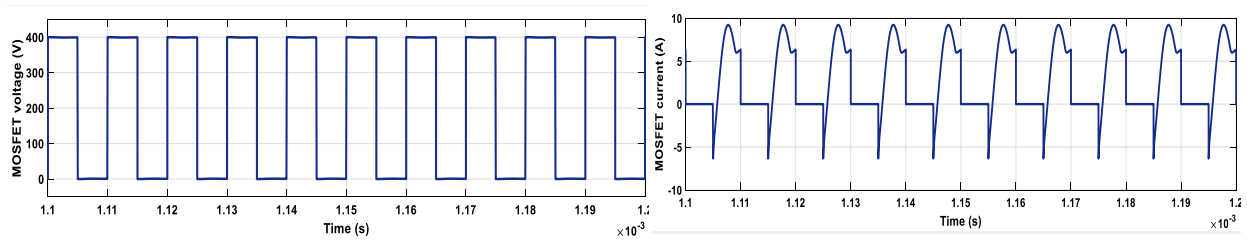


Figure 6. MOSFET voltage and current on the top a half-bridge converter

The resonant circuit's current envelope is illustrated in Figure (7). The current exiting the bridge inverter's output and passing through the inductor L_r is depicted in Figure (4.6)(a).

Due to the presence of harmonics, we determine that it is an alternating current that is close to the sinusoid. Corrugation occurs between $[-75, +75]$ amps.

In figure (7) (b), the current flowing through the magnetizing inductor L_m is depicted. We observe that it is similarly an alternating current but has fewer harmonics and is now rippling between $[-65, +65]$ amperes after being filtered by a value of 80 H.

In addition, the value of the curve's period is used to compute the resonant frequency at a value of 40 kHz. In this instance, the resonance frequency and the switching frequency of the MOSFETS are identical.

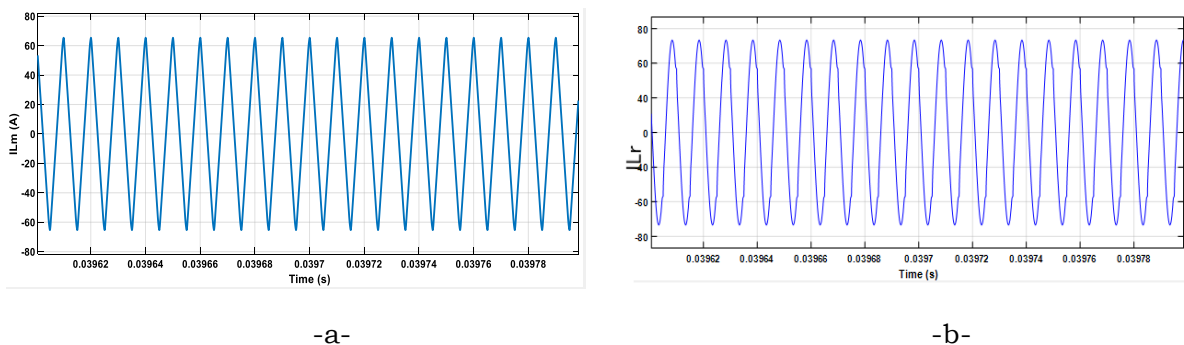


Figure 7. Currents in the resonance circuit a- $I_{Lr}(t)$ b- $I_{Lm}(t)$.

Figure (8) shows the voltage and current waveforms at the load (*t Leq*). The rectified voltage is measured around the value of 440 volts, and the current reaches approximately 14 amperes.).

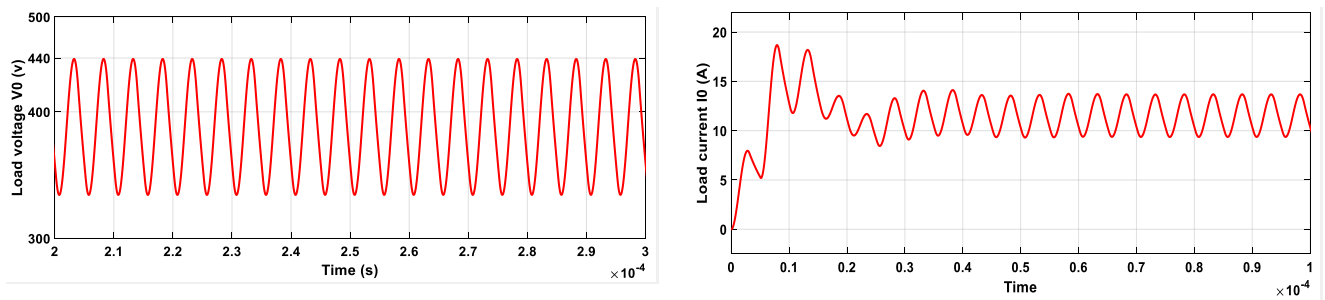


Figure 8. Output voltage and current Waveforms

From the above results, it is confirmed that the proposed scheme and assembly has good efficiency, and it is well suited for magnetic induction heating systems.

5. CONCLUSIONS

In this paper, simulation of induction heating offers a valuable approach to study and model the operation of a heating system before putting it into practice. This simulation makes it possible to virtually reproduce the real conditions, which makes it possible to evaluate the efficiency and the thermal behavior of the system. Using a complete mathematical and physical model, including components such as the inverter, the LLC resonant load, the rectifier transformer and the direct current load, the simulation makes it possible to understand the interaction of these elements and to generate an electromagnetic field which induces heat by induction. Key parameters such as inverter frequency, amperage and load geometry are analyzed to optimize energy efficiency and ensure even heat distribution. This simulation approach is therefore essential to improve the design and performance of induction heating systems.

REFERENCES:

- [1] Houam Ala , Fares Zaamouche, Djamel Ounnas ; (2022); The improvement of a grid-connected photovoltaic system output voltage quality by the variation of modulation index; 2nd International Conference in *industrial engineering and applied mathematics (isieam 2022)*. <https://test23.univ-skikda.dz/index.php/ar/actualites/62-international-seminar-in-industrial-engineering-and-applied-mathematics-isieam-2022>
- [2] Chao Huang, Yu Wang, Rui Zhong, Zhenkun Sun, Yonghui Deng, Lunbo Duan, (2023), Induction heating enables efficient heterogeneous catalytic reactions over superparamagnetic nanocatalysts, *Chinese Chemical Letters*, Volume 34, Issue 9, <https://doi.org/10.1016/j.ccllet.2022.108101>.
- [3] Jianliang Sun, Wenfan Zhang, Cunyao Shan, Lizhi Wang, (2023), Simulation and experimental research on local continuous induction heating of inner corrugated section, *International Communications in Heat and Mass Transfer*, Volume 147, <https://doi.org/10.1016/j.icheatmasstransfer>.
- [4] Kim, D.S., So, J.Y., Kim, D.K. (2016). Study on heating performance improvement of practical induction heating rice cooker with magnetic flux concentrator. *IEEE Transactions on Applied Superconductivity*,26(4):1-4.
<https://doi.org/10.1109/TASC.2016.2540650>
- [5] Sarnago, H., Lucia, O., Burdio, J.M. (2018). A versatile resonant tank identification methodology for induction heating systems. *IEEE Transactions on Power Electronics*, 33(3):1897-1901, <https://doi.org/10.1109/TPEL.2017.2740998>
- [6] Sreejyothi, K.R., Kumar, V., Chenchireddy, K., Tejaswi, P. (2022). Zero Voltage Switching (ZVS)-based DC-DC converter for battery input application. *AI Enabled IoT for Electrification and Connected Transportation*. https://doi.org/10.1007/978-981-19-2184-1_11
- [7] Vishnuram, P., Kumar, S., Singh, V.K., Babu, T.S., Kannan, R., Hasan, K.N.B.M. (2022). Phase shift- controlled dual-frequency multi-load converter with independent power control for induction cooking applications. *Sustainability*, 14(16): 10278.<https://doi.org/10.3390/su141610278>
- [8] Wenzhe Chen, Kangli Liu, Jianfeng Zhao, Cheng Jin, (2023), Dynamic improvement for phase-shift LLC resonant converter based on disturbance observer, *Energy Reports*, Volume 9, Supplement 1, Pages 1018-1025, <https://doi.org/10.1016/j.egyr.2022.11.115>.
- [9] Ngamrungsiri, H., Naetiladdanon, S., Sangswang, A. (2016). A variable-frequency asymmetrical voltage- cancellation control for inductive power transfer with series-series compensation. *13th International Conference on Electrical Engineering/Electronics, Computer, Telecommunications and Information Technology (ECTI-CON)*,pp. 1-6.
<https://doi.org/10.1109/ECTICon.2016.7561311>

[10] Balbi, H.D., Carrano, R.C., Passos, D. (2019). Revisiting probabilistic schedule-based asynchronous duty cycling. *Int J Wireless Inf Networks* 26, 24-38. <https://doi.org/10.1007/s10776-018-0420-5>

[11] Lee, J. H., Son, W. J., Ann, S., Byun, J., Lee, B. K. (2019). Improved pulse density modulation with a distribution algorithm for semi-bridgeless rectifier of inductive power transfer system in electric vehicles. 10th International Conference on Power Electronics and ECCE (ICPE 2019 - ECCE Asia), Busan, Korea (South),

[12] Wei, Y., Luo, Q., Mantooth, H.A. (2021). An LLC and LCL-T resonant tanks based topology for battery charger application. *CPSS Transactions on Power Electronics and Applications*, 6(4):263-275. <https://doi.org/10.24295/CPSSTPEA.2021.00025>

[13] Salem, M., Ramachandaramurthy, V.K., Jusoh, A., Sanjeevikumar, P., Kamarol, M., Teh, J., Ishak, D. (2020). Three-phase series resonant DC-DC boost converter with double LLC resonant tanks and variable frequency control. *IEEE Access*, 8(1): 22386-22399. <http://dx.doi.org/10.1109/ACCESS.2020.2969546>

[14] Zheng, J., Lu, S., Li, J. (2020). LLC and LCC analysis and comparison of resonant converters. In 2020 35th Youth Academic Annual Conference of Chinese Association Automation (YAC). <http://dx.doi.org/10.1109/YAC51587.2020.9337641>

[15] Patil, M., Choubey, R.K., Jain, P.K. (2022). Influence of coil shapes on temperature distribution in induction heating process. *Materials Today: Proceedings*. <https://doi.org/10.1016/j.matpr.2022.08.376pp.1-6> <https://doi.org/10.23919/ICPE2019-ECCEAsia42246.2019.8797336>

[16] CALLEBAUT Jean, « Chauffage par induction, Laborelec, Guide Power Quality Section 7»: Efficacité Energétique [www.leonardo-energy.org/France Edition Août 2007](http://www.leonardo-energy.org/France_Edition_Août_2007).

[17] Houam , A., Zaamouche, F., Ounnas, D. (2022). DPWM Applying for Five -Level NPC VSI Powered by PV-Boost Converter Based on Takagi Sugeno Fuzzy Model. *European Journal of Electrical Engineering* 24(2), 105-112. <https://doi.org/10.18280/ejee.240205>

[18] Houam Ala , Fares Zaamouche, Rabah Daouadi, Moussa Attia ; (2022); Efficiency Considerations of LLC Resonant Converter for Induction Heating Application; *European Journal of Electrical Engineering* ; 24(5-6):257-263; DOI: 10.18280/ejee.245-604.